PROCEEDINGS REPRINT

Reprinted from

Space Processing of Materials

4–5 August 1996
Denver, Colorado

P

Volume 2809

Evaluation of temperature gradient in Advanced Automated Directional Solidification Furnace (AADSF) by numerical simulation

Andris V. Bune [*], Donald C. Gillies [**] and Sandor L. Lehoczky [**]

[*] NRC Fellow, NASA MSFC, ES 75, Huntsville, AL 35812
[**] NASA MSFC, ES 75, Huntsville, AL 35812

ABSTRACT

A numerical model of heat transfer using combined conduction, radiation and convection in AADSF was used to evaluate temperature gradients in the vicinity of the crystal/melt interface for variety of hot and cold zone set point temperatures specifically for the growth of mercury cadmium telluride (MCT). Reverse usage of hot and cold zones was simulated to aid the choice of proper orientation of crystal/melt interface regarding residual acceleration vector without actual change of furnace location on board the orbiter. It appears that an additional booster heater will be extremely helpful to ensure desired temperature gradient when hot and cold zones are reversed. Further efforts are required to investigate advantages/ disadvantages of symmetrical furnace design (i.e. with similar length of hot and cold zones).

KEYWORDS: Furnace design, Numerical Modeling, Bulk Crystal Growth, HgCdTe, FIDAP

1. INTRODUCTION

In crystal growth by directional solidification, fluid flow is dominated in low gravity experiments by any residual acceleration vector, particularly a component transverse to the liquid-solid interface. The vector is due to an effect caused by the furnace not being at the center of mass of the orbiter, and the drag induced on the orbiter during flight. A high temperature gradient is essential in some crystal growth systems to achieve a growth rate comparable to convection driven fluid flow and still avoid constitutional supercooling. While the location of the AADSF may vary from mission to mission relative to the center of mass, there is generally a residual acceleration effect caused by the separation from the center of mass. The drag component has a magnitude and direction dependent on the flight orientation of the orbiter. To accommodate a variety of crystal growth systems on the same mission, in which the desired residual acceleration vector may have to point in opposite directions for optimum stability during growth, it might be necessary to fly the orbiter in two opposed directions. This may not be possible due to thermal concerns, safety concerns, communication concerns, etc. One possible solution to this problem is to exchange the hot and cold zones of the AADSF. AADSF has five zone heaters, and this paper describes the modeling simulation of the behavior and optimization of these heaters to achieve an acceptable temperature gradient with the hot and cold zones reversed. The advantages of having a

symmetrical heater furnace with booster heaters on both sides of the thermal barrier region are discussed.

It is well known that the temperature field in the vicinity of the crystal growth interface is a major factor responsible for the quality of crystals grown from the melt. In order to achieve complete control over the temperature field, special design features, such as multiple heaters, radiation shield and a heat extraction plate were incorporated into the design of the high gradient furnace built by Teledyne Brown Engineering for NASA [1] to implement directional solidification crystal growth on board the Space Shuttle. [2] Previous efforts have been made to determine, through numerical modelling, those thermal conditions for which HgCdTe crystal/melt interface shape is optimal, to ensure quality of crystal. [3,4,5] These works provide important insight on the problem, although only estimated temperature boundary conditions on the surface of the ampoule with HgCdTe were available. On the other hand numerical models of the global heat transfer in the AADSF furnace were developed. [1,6] In the present work these two approaches led to the joint model of the heat transfer in the furnace and of the melt convection during crystal solidification. Special consideration will be given to reverse usage of the hot and cold zones. Regarding the furnace modeling, the approach undertaken in the present work is close to that presented by Rosch. [6] However, in addition to conduction, both radiation and convection are directly included here in the numerical model. The advanced model of the sample that includes a realistic crystal/melt shape and realistic MCT properties is incorporated into the furnace model to represent actual growth experiment. The programming efforts were significantly reduced due to the use of the commercial finite element package FIDAP. [7]

2. AADSF NUMERICAL MODEL

The actual AADSF furnace design is shown schematically in figure 1. The design of the furnace includes five independently controlled heating elements to provide the desired temperature profile. The proposed additional booster heater is also indicated. Another important feature is the design of a steep temperature gradient zone which includes a booster heater, a heat extraction plate and insert to limit radiation transfer between the hot and cold zones. From a numerical modeling point of view, three typical zones in the furnace can be distinguished. First there is solid MCT along with molten material, where conduction and convection occur in an area with boundary movement caused by the solidification. There is no radiation in this area as MCT is opaque. Secondly, there are the fused silica ampoule, the surrounding furnace solid opaque parts, and empty cavities in which conduction and radiation are the primary modes of heat transfer. A brief description of the approach to model these two zones follows. Finally as the furnace cavities include argon, convection in the gas should be also taken into account. Although gas convection is actually incorporated into the furnace model, due to limitations on the size of the mesh this feature was not used in simulations presented here. It means that results of simulation represents microgravity conditions, rather then earth based experiment. On the other hand convection in the melt is included, to represent the effect of residual acceleration on board the orbiter. Conduction and radiation in furnace cavities are treated in the same way as in the rest of the furnace. Although the final results presented here are steady state temperature distribution, time dependence was included into the model, so that transient calculations could be performed to obtain a reasonable initial guess of the steady state finite element solution.
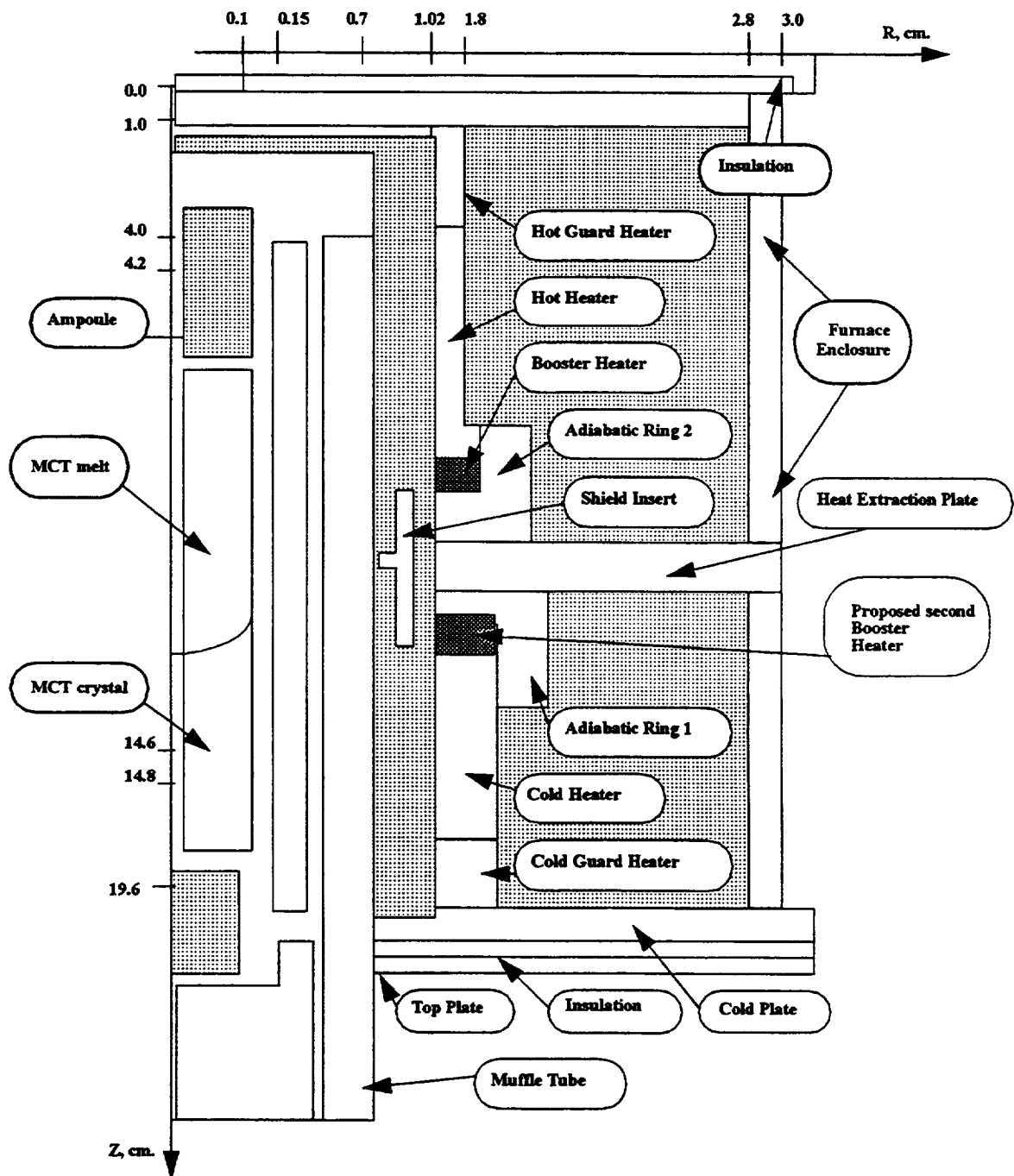
Figure 1. Schematic presentation of the AADSF furnace. Actual design with proposed second booster heater. Details of cartridge design are omitted.

3. Modelling of Conduction and Radiation

A numerical model proposed here is implemented throughout the furnace, as shown in figure 1. Necessary modifications are included in the area where convection occurs. The modeled area also include heating elements. In an actual experimental set up the temperature of each heating element is controlled via electronic control units to ensure that deviation from the desired set point temperature does not exceed 3.5° K, even for a maximum temperature of 1400°K. For this reason in the numerical model each heating element is assigned a constant set point temperature. To model this situation, one assumes there are no volumetric energy sources and that in the solid media heat transfer results from conduction only, such that

(1)

$$\rho C_p \frac{\partial T}{\partial t} = \nabla (k\nabla T)$$

Here ρ, C_p and k represents density, specific heat and conductivity of respectively. Appropriate boundary conditions include conduction and radiation

(2)

$$q_{total} = -n \cdot (k\nabla T) + q_{radiation}$$

To calculate the proper radiative heat flux $q_{radiation}$ that contributes to the total heat flux (2) radiative heat balance in each enclosure (cavity) must be considered. For this purpose the boundaries of enclosure can be treated as a set of M small areas, each area j with its own emissivity ε_j and surface temperature T_j. A new steady surface temperature distribution resulting from surface to surface radiation can be calculated using the enclosure equation.[7,8]

(3)

$$\sum_{j=1}^{M} \left(\frac{\delta_{i,j}}{\varepsilon_j} - F_{i,j} \frac{1 - \varepsilon_j}{\varepsilon_j} \right) q_{j, radiation} = \sum_{j=1}^{M} (\delta_{i,j} - F_{i,j}) \sigma_{SB} T_j^4$$

The view factors between two isothermal finite areas A_i and A_j can be calculated from

(4)

$$F_{i,j} = \frac{1}{A_i} \int_{A_i} \int_{A_j} \frac{\cos\theta_i \cos\theta_j}{\pi r_{i,j}} dA_i dA_j$$

To obtain radiation flux $q_{radiation}$ in boundary conditions (2) the sum over all finite radiating surfaces should be calculated.

$$(5)$$

$$q_{radiation} = -\sum_{j=1}^{M} q_{j, radiation} \qquad j \in A_j$$

Each enclosure presented in the model (totalling five) should be considered separately using equation (3) with related view factors (4). The numerical problem is now defined and can be solved using finite element technique implemented in FIDAP package.[7]

4. Convection, Conduction and Solidification.

In the molten material, equation (1) should be modified to incorporate convection

$$(6)$$

$$\rho C_p \left(\frac{\partial T}{\partial t} + u \cdot \nabla T \right) = \nabla (k \nabla T)$$

Molten MCT is considered as an incompressible fluid, with laminar flow due to buoyancy force. The density variation is included in the momentum conservation equation, but density is set constant elsewhere in accordance with Boussinesq approximation.

$$(7)$$

$$\rho \left(\frac{\partial u}{\partial t} + u \cdot \nabla u \right) = -\nabla p + \mu \cdot \Delta u + \rho g \left[1 - \beta (T - T_0) \right] \qquad \nabla \cdot u = 0$$

The phase change interface is considered as free (moving) boundary. Species transport across the interface is not incorporated at this time. The following set of boundary conditions apply. First, the melting temperature should be preserved on solid/melt interface

$$(8)$$

$$T_{melt} = T_{solid} = const$$

Heat transfer balance on the interface should include solidification latent heat release, L.

$$(9)$$

$$k_{solid} \nabla T_{solid} \cdot n - k_{melt} \nabla T_{melt} \cdot n = \rho L \frac{dS_{solid}}{dt}$$

The new independent variable S represents the location of solid/melt boundary. Balance of the mass across interface should be preserved so that

$$(10)$$

$$\rho_{melt} \frac{dS_{melt}}{dt} = \rho_{solid} \frac{dS_{solid}}{dt}$$

No-slip boundary conditions are applied

$$u_{melt}(S) = 0$$

To resolve this problem the moving boundary feature of the finite element code FIDAP was used. [7]

5. TEST PROBLEM

In order to verify modelling approach as well as numerical procedures the following problem previously investigated both numerically and experimentally in reference[9] was considered. Combined conduction, radiation and gas convection due to side wall temperature difference occur in a square enclosure in a piece of solid material (lexan). The results of 2-D test run presented on figure 2. indicate good agreement with the findings of Kim and Viskanta.[9]
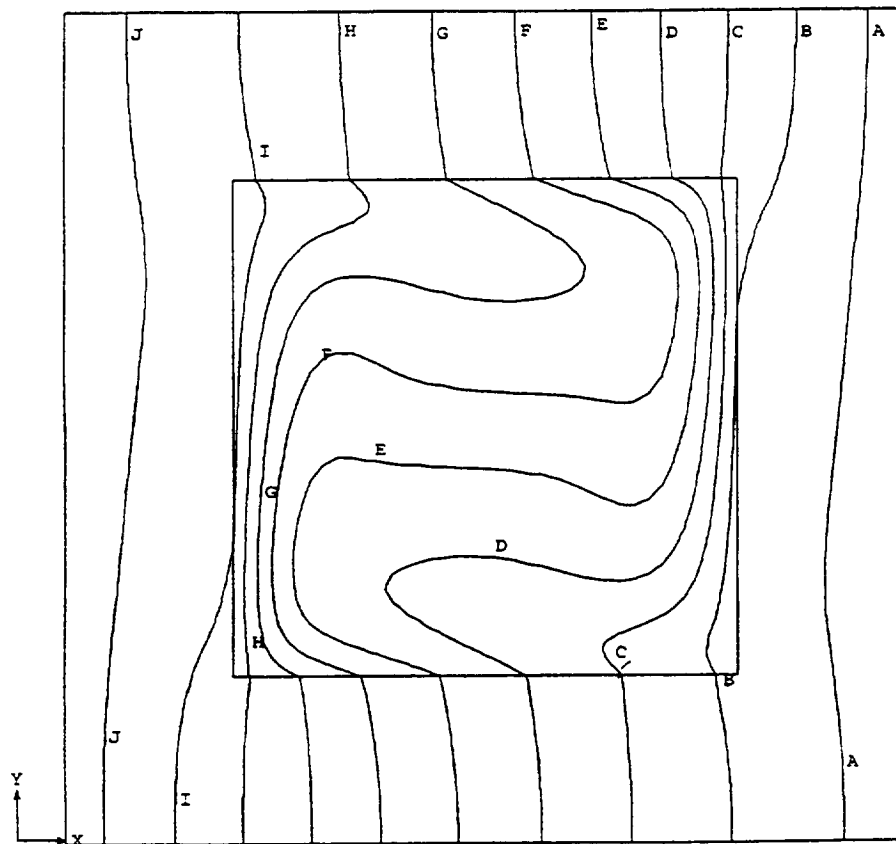

Figure 2. Combined conduction, radiation and convection in enclosure. Temperature field in the cavity filled with air and in solid wall (lexan) The isotherms marked A corresponds to 270.6°K, B-275.8°K, etc., J-317.4 °K.

6. RESULTS

Typical results of simulations are presented in figure 3. The steady state temperature field in furnace shown was obtained for the following temperature set points: 330^0C, 360^0C, 854^0C, 846^0C, 856^0C for cold guard, cold, booster, hot and hot guard heaters respectively, that is referred as case 1 in table 1. A remarkable feature of temperature distribution is the practically linear temperature profile on the outer boundary of the furnace, as well as on the axis of the furnace, so that the gradient in the ampoule vicinity is higher. It is shown that better insulation below and above the ampoule and crystal, such as usage of ceramic blanket to fill in empty spaces, results in a higher temperature gradient. The effect of the shield insert is clearly indicated, as it almost completely blocks radiative heat transfer from booster heater to the cartridge. The heat extraction plate has a practically constant temperature, due to the high conductivity of material (inconel) up to 23.2 J/m-s-K at 1144.25^0K, staring from 10.7J/m-s-K at 477.55^0K. In the present study the global modeling of furnace is used to provide realistic temperature boundary conditions for crystal growth zone. When both crystal and melt are incorporated into a global model of furnace, it appears that sufficient resolution of solid/melt interface requires a fine mesh presently available only in a separate complementary model. Due to this limitation solutal convection and effects of double-diffusion were neglected here. The thermophysical properties of HgCdTe are similar to used in work [4], except the viscosity. Recently measured temperature dependent viscosity data from [10] were used. A summary of the cases considered numerically is presented in table 1.

TABLE 1.

Set temperature	Case 1	Case 2	Case 3	Case 4
Cold Guardian	330^0C	330^0C	856^0C	856^0C
Cold Heater	360^0C	360^0C	846^0C	846^0C
Proposed additional booster heater	N/A	set free	N/A	854^0C
Booster Heater	854^0C	854^0C	set free	set free
Hot Heater	846^0C	846^0C	360^0C	360^0C
Hot Guard	856^0C	856^0C	330^0C	330^0C

The calculation of the gradient close to the interface in both the melt and the solid can be made from consideration of temperature field presented on figure 3 for case 1 and the analogous figures for the other three cases. So do this with high degree of confidence, however, requires that a much finer mesh be applied locally. this work is on-going.
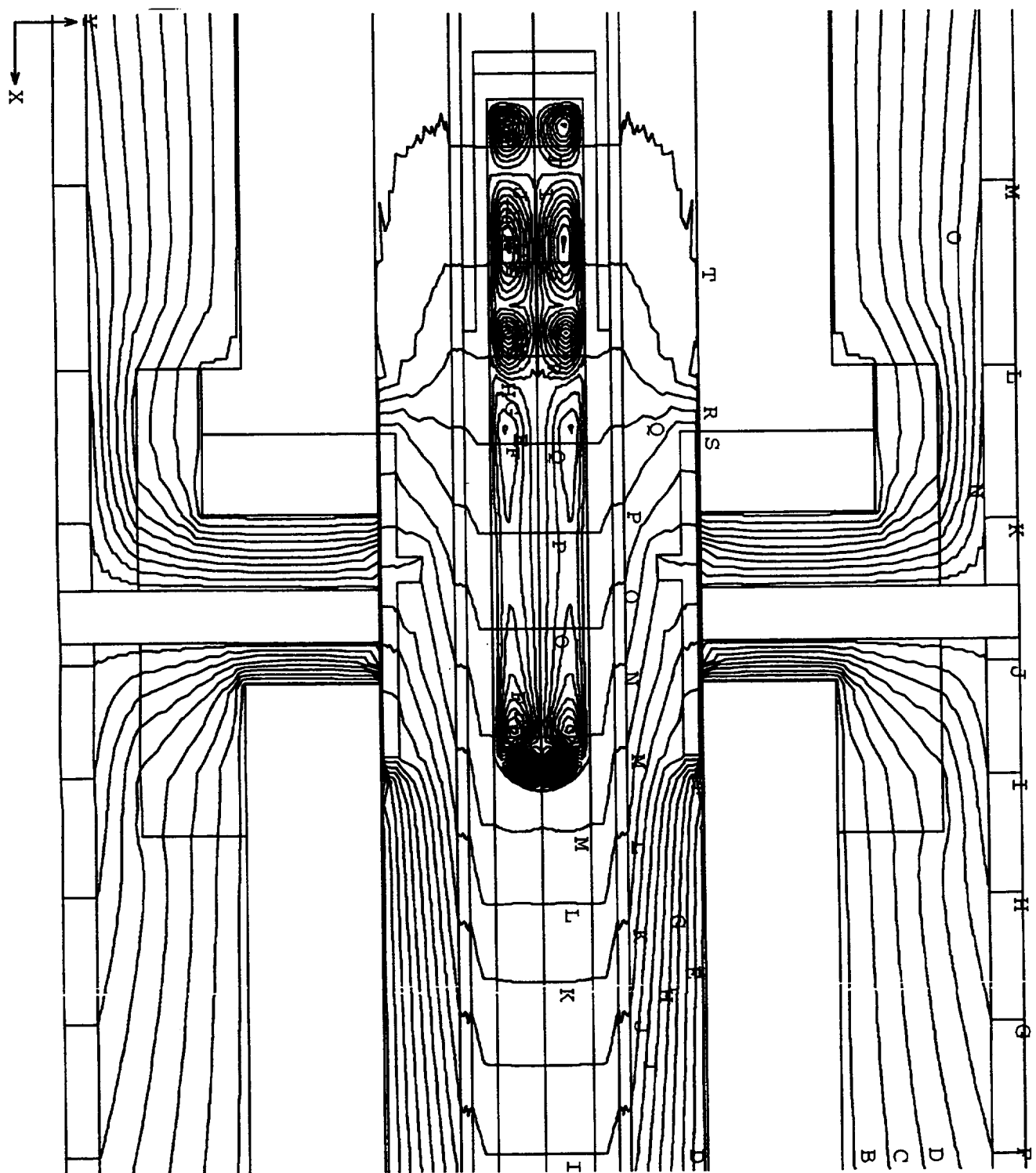
Figure 3. Temperature field in central part of the furnace.The isotherms marked B corresponds to 642.6°K, C-668.9°K, etc., T-1116°K.The isotherms are spaced at 26.3°K. Streamlines indicate location of molten MCT.

7. CONCLUSIONS

A realistic model of heat transfer in AADSF was used to evaluate temperature gradients in the vicinity of the crystal/melt interface for a variety of heaters set temperatures. It indicates, that reverse usage of furnace cold and hot zone, to ensure proper orientation of crystal/melt interface relative to the residual acceleration vector on orbiter without changing the actual location of the furnace can be achieved. The additional booster heater will be extremely helpful to maintain desired temperature gradient. Further efforts are required to investigate advantages/ disadvantages of symmetrical furnace design (i.e. with similar length of hot and cold zones).

8. ACKNOWLEDGMENTS

9. REFERENCES

1. J. LeCroy and D. Popok, AIAA 94-0336, 32rd Aerospace Sciences Meeting and Exhibit, Reno, NV, January 1994.

2. S.L. Lehoczky, D.C. Gillies, F.R. Szofran, F.A.Reeves, J.D.Sledd, J.M.Cole, T.K.Pendergrass, D.A. Watring, C.R. Coppens, J. LeCroy and D. Popok,"Crystal Growth of HgCdTe in the AADSF on the USMP-2 Mission" AIAA 95-0609, 33rd Aerospace Sciences Meeting and Exhibit, Reno, NV, January 1995.

3. R.J. Naumann and S.L. Lehoczky, "Effect of Variable Thermal Conductivity on Isotherms in Bridgman Growth"J. Crystal Growth, Vol. 61, pp. 707-710, 1983.

4. D.H.Kim and R.A.Brown,"Modelling of the dynamics of HgCdTe growth by vertical Bridgman method" J. Crystal Growth, Vol. 114, pp. 411-434, 1991.

5. Yu.V.Apanovich and E.D. Ljumkis, "The numerical simulation of heat and mass transfer during growth of a binary system by travelling heater method"J. Crystal Growth Vol. 110,pp. 839-854, 1991.

6. W.R. Rosch, *Furnace Temperatures and Their Effect on Vertical Bridgman Crystal Growth* Ph.D. thesis, University of Virginia, 1995.

7. *FIDAP Theory Manual*, Version 7.0, Fluid Dynamics International, Inc., Evanston, IL, 1993.

8. R.Siegel and J.R.Howell, *Thermal Radiation Heat Transfer*, 2nd ed., pp.172, 331-339, 607-609, McGraw-Hill, New York, 1981.

9. D.M. Kim and R.Viskanta,"Effect of Wall Conduction and Radiation on Natural Convection in a Rectangular Cavity" Numerical Heat Transfer Vol.7, pp. 449-470, 1984.

10. K. Mazuruk, C.-H. Su, S.L. Lehoczky and F. Rosenberger,"Novel oscillating cup viscometer - application to molten HgTe and $Hg_{0.8}Cd_{0.2}Te$", J.Appl.Phys., Vol. 77 (10), pp. 5098-5102, 1995.